PHYSICAL REVIEW A VOLUME 36, NUMBER 10 NOVEMBER 15, 1987

Deconvolution and characteristics of cusp spectra for electron transfer to the projectile's continuum (ETC): Extraction of a generic cross section

Y. C. Yu* and G. Lapicki
Department of Physics, East Carolina University, Greenville, North Carolina 27858
(Received 20 October 1986; revised manuscript received 21 May 1987)

Observed cusp spectra for electron transfer to the continuum (ETC) of 0.6-MeV/u H^+, He^+, and He^{2+} ions from hydrocarbon gaseous targets (CH_4, C_3H_6, and C_7H_{16}) are fitted to a generic expression of Meckbach, Nemirovsky, and Garibotti [Phys. Rev. A **24**, 1793 (1981)]. Six leading terms of this formula are given here analytically. They were derived after the convolution of the assumed expression for the ETC cross section with an analytical function that accounts for the electron transmission through the electron spectrometer of specified longitudinal and transverse velocity resolution. With given angles that determine the angular acceptance as instrumental parameters, formulas for these terms are expressed as universal functions of a single variable which is the ratio of electron speed v to ion speed v_i. The least-squares fit of these functions to experimental cusps allows for reconstruction of the generic ETC cross section, which is not "polluted" by finite resolution of the electron spectrometer. Key characteristics, the asymmetry and relative width of deconvoluted cross sections, are discussed. The skewness in observed cusp spectra is traced to the scattering angles that, relative to the spectrometer's half-angle of acceptance θ_0, are small; this is particularly seen in electron capture to continuum (ECC) data, while the spectra dominated by electron loss to continuum (ELC) are more symmetric and less dependent in their asymmetry on the scattering angle θ. The relative full widths at half maximum, $(\Delta v/v)_{\mathrm{FWHM}}$, for the deconvoluted ECC cross sections rise significantly faster with the increasing θ than for the ELC cross sections; this difference is obscured in observed cusp spectra by the finite velocity resolution of the spectrometer. Relatively narrow resolution results in the preferential detection of the highly forward scattered electrons whose velocity distribution conforms with the leading term, $1/|\mathbf{v}-\mathbf{v}_i|$, for ETC cross sections. Hence, for all projectile-target combinations, the observed spectra have the relative widths which are of comparable magnitude and in very good agreement with Dettmann's prediction, i.e., $1.5\theta_0$. A comment on wakes as possible contributors to cusps observed in ETC from large hydrocarbon molecules is made.

I. INTRODUCTION

The velocity spectrum of electrons, ejected into the forward direction in the aftermath of ion-atom collision, exhibits a cusp-shaped peak when the electron velocity $\mathbf{v}$ matches the ion velocity $\mathbf{v}_i$. The etiology of this cusp is attributed to electron transfer into the projectile's ion continuum (ETC). The ETC can occur by various mechanisms of which the electron capture and loss are the most prominent processes. When the transferred electron originates from the target atom, the projectile can capture the electron into its continuum; this particular ETC process is known as the electron capture to the continuum (ECC) and it is the dominating process when the projectile is a fully stripped ion. In addition to the ECC contribution to the electron cusp, partially stripped ions may shed their electrons in the electron-loss processes to their own continuum (ELC). Moreover, in solid targets a narrow component of the electron cusp has been isolated[1] as a signature of an ETC from a wake state that develops behind the projectile. This observation has stimulated others to search for the existence of a narrow component in ETC spectra from molecular targets;[2] the emergence of this component with the increasing complexity of the molecules and lack of any alternate consistent explanation, confirmed, in fact, that wake formation in molecules of a sufficiently large extension is possible.[3]

Since the discovery[4] of the electron cusp there has been an undiminished interest in its nature, both experimentally and theoretically, as documented in several reviews on ETC.[5] Earlier theories viewed the ECC process in terms of a first-order perturbation approach to the electron exchange amplitude and predicted a nearly symmetry cusp. Experiments for bare heavy projectiles[6] and even for light hydrogenic projectiles[7] resulted, however, in an ECC peak that was skewed in shape toward lower electron velocities. This skewness has been explained in the second-order Born approximation, in which transferred electrons are distorted by the ion.[8] No significant asymmetries, as expected in the Born approximation, were found in the cusps that were primarily traceable to ELC.[9] Symmetrical cusps were indeed seen in bombardment by partially stripped heavy ions,[10] although light and singly ionized ions exhibit certain asymmetry in the cusp peaks.[11]

Characteristics of experimental cusp spectra, such as asymmetry and width, are in part determined by instrumental resolution of the electron spectrometer used in the specific experimental arrangement. In this work we review a modification[12] to the procedure[13] that was introduced and developed for deconvolution of such spectra so that an ETC cross section $d^2\sigma/dv\,d\theta$— doubly differential in the electron speed and angle of scattering—could be extracted from the data. To ensure a general utility of the Meckbach *et al.* method,[13] we expand $d^2\sigma/dvd\theta$ into the six terms that are expected[14–16] to shape the cusplike spectrum.[13] The novelty of our approach lies in an *analytical* convolution of these terms with chosen instrumental resolution functions so that the expansion terms, which represent the deconvoluted ETC cross section, can be easily extracted from experimental spectra. This procedure differs from the established technique[13–16] that fits the data to a number of expressions, which are constructed through numerical evaluations of a double integral for each term and with standard, albeit cumbersome, nonlinear least-squares programs. We extract $d^2\sigma/dv\,d\theta$—which can then be meaningfully discussed vis-á-vis theories and direct experiments for this doubly differential ETC cross section—by a least-squares fit of our analytical functions to the observed spectra.

In Sec. II analytical approximations to the spectrometer's electron velocity resolution and angular acceptance functions are made so that formulas for convoluted $d^2\sigma/dv\,d\theta$ can be derived. These formulas were presented in Appendixes B and C of Ref. 12. After notational modifications and removal of misprints in Ref. 12, they are reproduced in the Appendix of this paper. In Sec. III, through numerical fits to the experimental cusps, we extract the coefficients with which the expansion terms—whose sum convolutes to the observed yields—contribute to deconvoluted ETC cross sections. Key characteristics, the asymmetry and the relative width, of these cross sections are discussed in Sec. IV. Section V concludes this paper.

II. INSTRUMENTAL TRANSMISSION FUNCTION

Electrons, generated in electron transfer to the continuum processes with the cross section $d^2\sigma/dvd\theta$, are detected through an electron spectrometer. The measured electron yield Y is a convolution of this cross section with the spectrometer's transmission function T for electrons of velocity $\mathbf{v}$,

$$Y=\int T(\mathbf{v})\,d^2\sigma/dv\,d\theta\,d^3v\ , \tag{1}$$

where $d^3v=v^2dv\,\sin\theta d\theta d\phi$ is the volume element in the electron velocity space into which the transferred electrons are scattered. The kinematics of this process is pictured in Fig. 1. Since $d^2\sigma/dvd\theta$ diverges when $\mathbf{v}\rightarrow\mathbf{v}_i$ ($\mathbf{v}'=\mathbf{v}-\mathbf{v}_i\rightarrow 0$), experimental resolutions [i.e., the acceptance of produced electrons in electron speed v (or energy $E=v^2/2$ in atomic units) and in solid angle $d\Omega=\sin\theta d\theta d\phi$] are decisive in determining the measured shapes and widths. These acceptances are represented in Fig. 1 approximately by a cylindrical

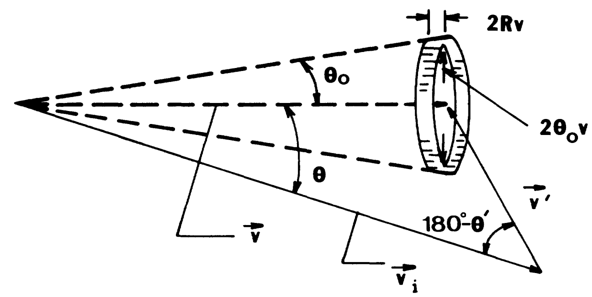

FIG. 1. The electron $\mathbf{v}$ minus the ion $\mathbf{v}_i$, velocity difference $\mathbf{v}'=\mathbf{v}-\mathbf{v}_i$, is shown to illustrate the kinematics of the forward scattering in the velocity space. θ and θ' are scattering angles of the transferred electron in the rest and moving frames of the ion. For definitions of θ_0 and R see text.

"resolution volume"[13] of height $2Rv$ and diameter $2\theta_0 v$. Note the cylinder radius is obtained from $v\tan\theta_0$ in the small-angle approximation (which is valid when θ_0 is a few degree angle), while the cylinder height represents Δv taken as full width at half maximum (FWHM). $R=(\Delta v/v)_{\mathrm{HWHM}}$ is the experimental relative resolution in the electron speed; note that R is half of the experimental relative resolution in the energy spectrum of a spectrometer, $(\Delta E/E)_{\mathrm{HWHM}}=2R$. The angle θ_0 is the half-angle of the spectrometer's angular acceptance cone. R and θ_0 set the limits for longitudinal and transverse velocity resolutions, respectively.

ETC electrons are emitted in a forward cone that has a perfect azimuthal symmetry in the angle ϕ, the symmetry which is unspoiled by spherical electron spectrometers. As we restrict our discussion to data taken with a spherical electron spectrometer, it is only the finite angular acceptance function $\Theta(\theta)$ and a limited electron speed resolution—as defined by the spectrometer's transmission function $V(v)$—that will ultimately shape the measured output as the observed electron spectrum. One usually assumes[13] that the overall transmission function can be taken as a product of the speed and angular function, i.e., $T(\mathbf{v})=V(v)\Theta(\theta)$. With this separation of variables in the azimuthally independent T, Eq. (1) gives

$$Y=2\pi\int_0^{\pi}\Theta(\theta)\int_0^{\infty}V(v)\,d^2\sigma/dv\,d\theta\,v^2dv\,\sin\theta\,d\theta\ , \tag{2}$$

where, by the mean-value theorem, $d^2\sigma/dv\,d\theta$ is essentially undistorted by the electron speed dispersion in the electron spectrometer of a sufficiently small R. With the leading term of $d^2\sigma/dv\,d\theta$ proportional to $1/|\mathbf{v}-\mathbf{v}_i|$, this cross section has a cusp at $\mathbf{v}=\mathbf{v}_i$ where the cross section becomes a singular function of v at $\theta=0°$. Notwithstanding the singularity of $d^2\sigma/dv\,d\theta$, the integrand of Eq. (2) involves $\sin\theta d^2\sigma/dv\,d\theta$ which is analytic. Its dominating term, $\sin\theta/|\mathbf{v}-\mathbf{v}_i|$, converges to $1/v_i$ as $\sqrt{(1+\cos\theta)/2(1\pm R)}/v_i$ when $R\ll 1$. At $\theta=0°$ in particular, $\sin\theta/|\mathbf{v}-\mathbf{v}_i|$ $\sqrt{(1\pm R)}/v_i$ in the small neighborhood around $v=v_i$. Thus a Taylor-series expansion of this integrand around the center of the $[v(1-R),v(1+R)]$ interval is admissible even at $\theta=0°$. The convergence of the series is required only on this interval; the HWHM of $V(v)$ suffices as the radius of convergence for this series. In the $R \ll 1$ limit, each term of the series expansion—independently of θ—integrates to its value at v multiplied by a common factor of $2v^3R$. Thus in the $R \to 0$ limit, Eq. (2) transforms effectively into

$$Y = 2\pi \int_0^\pi \Theta(\theta)\, d^2\sigma/dv\, d\theta \sin\theta\, d\theta \int_0^\infty V(v) v^2 dv \ . \quad (3)$$

It should be noted that Eq. (3) derives from Eq. (2) at any angle θ; in particular, it is not necessary that R should be smaller than the half-angle of acceptance θ_0 as long as $R \ll 1$. In many observations of cusp spectra, including the data to be analyzed in this work, R is comparable to θ_0 and yet the cardinal requirement of small R is well satisfied. For the simplest choices of the $V(v)$ function, a rectangle and a triangle of identical heights and widths at half maximum, one obtains respectively, $2v^3R(1+R^2/3)$ and $2v^3R\ (1+2R^2/3)$. With $R \ll 1$, which is characteristic of electron spectrometers, both rectangular and triangular windows of equal area filter through identical volume of electrons, $2v^3R = v^2\Delta v$, in the electron velocity space.

An experimentally determined angular acceptance function, $\Theta(\theta)$, has typical behavior as shown in Fig. 2. The angle θ is measured with respect to the principal axis of the spectrometer which, since one measures forward-emitted electrons, coincides with the direction of the ion beam. If all electrons were to originate from the same point, a distance d in front of the spectrometer's entrance window of width w, then the $\Theta(\theta)$ would be given by a step function that vanishes for angles larger than the conventional half-angle of acceptance $\theta_0 = \tan^{-1}(w/2d)$. Experimental calibration of electron points (see Fig. 3 of Ref. 13) points to a less abrupt change of Θ from 1 to 0 in the vicinity of θ_0. We attribute this to a finite spatial extension from which the electrons are accepted into the spectrometer. The following two characteristic angles are introduced: θ_1, the angle below which all electrons are accepted and θ_2, the angle above which none of the electrons can enter the spectrometer. Finite dimensions of the cell region from which ETC electrons originate—l taken longitudinally along principal axis of the spectrometer and t being its size measured transversely to it —define $\theta_1 = \tan^{-1}[(w/2 - t/2)/(d - l/2)]$ and $\theta_2 = \tan^{-1}[(w/2 + t/2)/(d - l/2)]$ which converge to θ_0 only in the $t \ll w$ and $l \ll d$ limits (see Fig. 1 of Ref. 12).

We have considered the following analytical approximations to simulate experimental $\Theta(\theta)$ with an increasing accuracy. As the measured Θ appeared to equal $\frac{1}{2}$ at $\theta_0 = (\theta_1 + \theta_2)/2$ (Ref. 13), we considered simple functions that satisfied this condition and were equal to 1 and 0 for $\theta < \theta_1$ and for $\theta > \theta_2$, respectively. A step function $\Theta = 1$ for $\theta < \theta_0$ and 0 for $\theta > \theta_0$, which on the average equals $\frac{1}{2}$ at θ_0, was the simplest choice. However, in the neighborhood of θ_0, the step function overestimates the experimental angular acceptance function for $\theta < \theta_0$ (and it underestimates the experimental Θ for $\theta > \theta_0$) too severely. A triangular approximation, $\Theta = (\theta_2 - \theta)/(\theta_2$

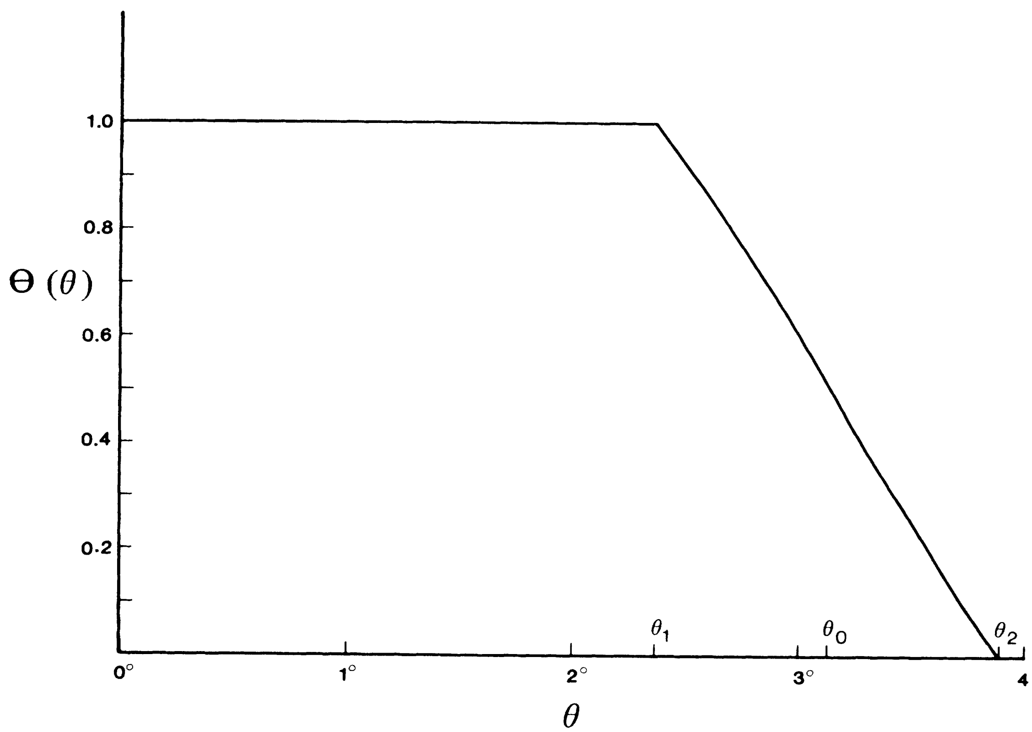

FIG. 2. Angular acceptance function for an electron spectrometer. The curve is drawn according to Eq. (4) which is utilized in our work as a realistic and analytical form for Θ. This curve was calculated with $\theta_1 = 2.36°$ and $\theta_2 = 3.88°$ that correspond to the instrumental arrangement in which the provided[18] data were gathered.

$-\theta_1$) in the $\theta_1 \leq \theta \leq \theta_2$ range, still appears to be unsatisfactory. A quadratic form for Θ could not be fit given our restrictions. A polynomial of at least third degree in θ would have been required; the θ integration in Eq. (3) would amount to four types of integrals. Two of them due to the θ and θ^3 terms are elliptic integrals, which would be very inconvenient for further use in numerical fits of the electron spectra. Thus we introduce Θ as

$$\Theta = \begin{cases} 1, & \theta \leq \theta_1 \\ a_0 + a_1\cos\theta + a_2\cos^2\theta, & \theta_1 \leq \theta \leq \theta_2 \\ 0, & \theta \geq \theta_2 \end{cases} \tag{4}$$

with $a_0 + a_1\cos\theta_i + a_2\cos^2\theta_i = \delta_{i1}$ $(i=1,2)$, to satisfy the continuity of Θ at θ_i, and with $a_0 + a_1\cos\theta_0 + a_2\cos^2\theta_0 = \frac{1}{2}$ so that the experimental behavior of Θ is accurately mimicked. An expansion of Θ into powers of $\cos\theta$ allows further integrations in Eq. (3) to be performed analytically as it was done in Appendixes B and C of Ref. 12; the termination of the expansion at $\cos^2\theta$ term suffices to reproduce the experimental angular acceptance of an electron spectrometer [see the curve according to Eq. (4) in Fig. 2 and compare it with Fig. 3 of Ref. 13]. Given the three constraints imposed on Θ of Eq. (4), the coefficients a_0, a_1, and a_2 can be easily found by Gaussian elimination for fixed values of θ_1 and θ_2. Explicitly in terms of $\mu_i \equiv \cos\theta_i$ $(i=0,1,2)$, $a_2 = (\mu_0 - \mu_1/2 - \mu_2/2)/[(\mu_1-\mu_2)(\mu_1-\mu_0)(\mu_0-\mu_2)]$, $a_1 = 1/(\mu_1-\mu_2) - a_2(\mu_1+\mu_2)$, and $a_0 = -\mu_2(a_1+\mu_2 a_2)$.

III. FITTING OBSERVED CUSP SPECTRA

Inspired by predictions of Dettmann[17] for ECC cross sections, as well as by later treatments of the ELC process, Meckbach and co-workers[13] proposed to expand $d^2\sigma/dv\,d\theta$ into a finite series

$$d^2\sigma/dv\,d\theta = \frac{1}{v'}\sum_{n,l} B_{nl}\left[\frac{v'}{v_i}\right]^n P_l(\cos\theta') , \tag{5}$$

where $v' = (v^2 + v_i^2 - 2vv_i\cos\theta)^{1/2}$ and $\cos\theta' = (v\cos\theta - v_i)/v'$ are the electron speed and scattering angle in the frame of the ion moving with a speed v_i. Figure 1 shows their relation to v, v_i, and θ in the laboratory frame in which the cross section $d^2\sigma/dv\,d\theta$ of Eq. (5) is measured. In Eq. (5) we have departed from Eq. (6) of Ref. 13: v' under the sum has been replaced with v'/v_i so that—irrespectively of any chosen units of velocity—both the $n=0$ and $n=1$ B_{nl} coefficients will always have the same units of the cross section.

The leading term ($n=0$ and $l=0$) in this expansion accounts principally for the singularity of $d^2\sigma/dvd\theta$ as $v' \rightarrow 0$; the Legendre polynomials P_l with $l>0$ allow for possible deviations ETC cross sections from the spherical symmetry in the v' space. B_{nl} in Eq. (5) were[13] the electron velocity independent coefficients; fixed for given velocity v_i and type of projectile, they are to be obtained from a fit to the experimental cusp spectra. The relative magnitudes of various terms in Eq. (5) were considered significant to ascertain their importance as they characterize deviations of observed spectra from a simple spherically symmetric shape around v'. Equation (5) employs a generic formula for $d^2\sigma/dvd\theta$ of Eq. (5) in the sense that it describes a general class of cross sections characterized by the prominent forward peak; its specificity can be only established when ETC is dominant by an exclusive mechanism. For the ion beam of fixed velocity v_i and the spectrometer characterized by θ_1 and θ_2, one obtains the ETC yield spectrum

$$Y(v;v_i,\theta_1,\theta_2) = \sum_{n,l} B_{nl}(v_i) U_{nl}(v;v_i,\theta_1,\theta_2) \tag{6}$$

as a function of the detected electron velocity v. The expansion terms

$$U_{nl} \equiv (4\pi R v^3/v_i) \int_0^\pi \left[\frac{v'}{v_i}\right]^{n-1} P_l(\cos\theta')\Theta(\theta)\sin\theta d\theta \tag{7}$$

were evaluated by Meckbach *et al.*[13] *numerically* using a rather primitive step function approximation to Θ. To make the Meckbach *et al.* method more versatile, we have presented[12] analytical functions for U_{nl} that—to force this method to conform with a more realistic acceptance function—are based on Θ of Eq. (4). Formulas for U_{nl} are reproduced in the Appendix. Our procedure allows for a straightforward comparison of theories for ETC processes with a reconstructed $d^2\sigma/dv\,d\theta$ of Eq. (5), rather than with the observed cusp of Eq. (6). The experimental yield for electrons transferred to the projectile's continuum in the detected spectra is veiled by instrumental distortions that seriously obscure the clarity of conclusions about the asymmetry and width characteristics of ETC cross sections.

Meckbach *et al.*[13] truncated Eq. (6) to four terms with the lowest indices n and l, i.e., with $n=0,1$ and $l=0,1$. Berry *et al.*[14] have extended the l summation up to the $l=2$ terms. The recent fits[15] indicate that these "d-like" terms are relatively insignificant for the fit quality. Such inferences stem, however, from analyses of the cusp spectra obtained from $He^+, He^{2+} \rightarrow$ He collisions; the $l=2$ terms could be important in the asymmetric collisions that were analyzed in Refs. 13 and 14. Andersen *et al.*[16] use the $n=1$ terms to fit their H^+, $He^{2+} \rightarrow$He data, but dismiss these terms as inaccurate. They argue that the $n=1$ terms, probing the character of observed spectra in the wings, do not clearly associate with ETC production because an underlying contribution of direct ionization surfaces in the cusp wings. This obstruction due to direct ionization could indeed be significant in symmetric or nearly symmetric collision systems. In more asymmetric collisions, such as for the data that we will analyze, direct ionization is expected to be a lesser contributor to the observed spectra. Thus we have fitted[12] the provided $H^+, H^{2+} \rightarrow C_nH_m$ electron yields[18] to a six-term expansion,

$$Y = B_{00}U_{00} + B_{01}U_{01} + B_{02}U_{02} + B_{10}U_{10} + B_{11}U_{11} + B_{12}U_{12} , \tag{8}$$

which *a priori* was believed to entail the main ETC contributors to the cusp.

As a test case for our procedure, we have chosen to analyze spectra obtained at East Carolina University (Ref. 18) in electron transfer from various hydrocarbons by protons and helium ions of the same velocity in 0.6-MeV/u beams. Spectra obtained with singly as well as with doubly ionized helium were analyzed because the He^+ data were expected to be a manifestation of the ELC process, while the He^{2+} data— as well as the proton-induced spectra—were anticipated due to the ECC mechanism. Moreover, molecular targets offered a possibility of detecting a wake contribution which prompted us to focus on CH_4 versus C_7H_{16} to check if molecules of different sizes generate, ceteris paribus, spectra that differ because wakes could develop in larger molecules. The specifics of the the size and location of the target cell, from which ETC electrons enter into the spherical 160° sector electron spectometer, are listed in Appendix A of Ref. 12. They serve as an input in analytical evaluation of U_{nl}.

Figure 3 shows $U_{nl}/4\pi R v^2$ terms of Eq. (8) calculated for the provided data according to the formulas derived in Appendixes B and C of Ref. 12 and listed in the Appendix of this paper. For an easy recognition of the s, p, and d-like origin of these terms, we denote them as $S_0=U_{00}/4\pi R v_i^2$, $P_0=U_{01}/4\pi R v_i^2$, $D_0=U_{02}/4\pi R v_i^2$, $S_1=U_{10}/4\pi R v_i^2$, $P_1=U_{11}/4\pi R v_i^2$, and $D_1=U_{12}/4\pi R v_i^2$. The subscript of the S_n, P_n, and D_n functions distinguishes between $n=0$ and $n=1$ terms in the $(v'/v_i)^n$ expansion of Eq. (5). The $n=1$ terms were multiplied in Fig. 3 by a factor of 10 to exhibit them more clearly. For a broad intercomparison of the S_n, P_n, and D_n functions, they are shown over a wide x interval from 0.8 to 1.2 in Fig. 3; they were utilized to fit the analyzed spectra, however, over the $0.9 \le x \le 1.1$ range. These functions are independent of the velocity resolution and depend parametrically on the angles that define

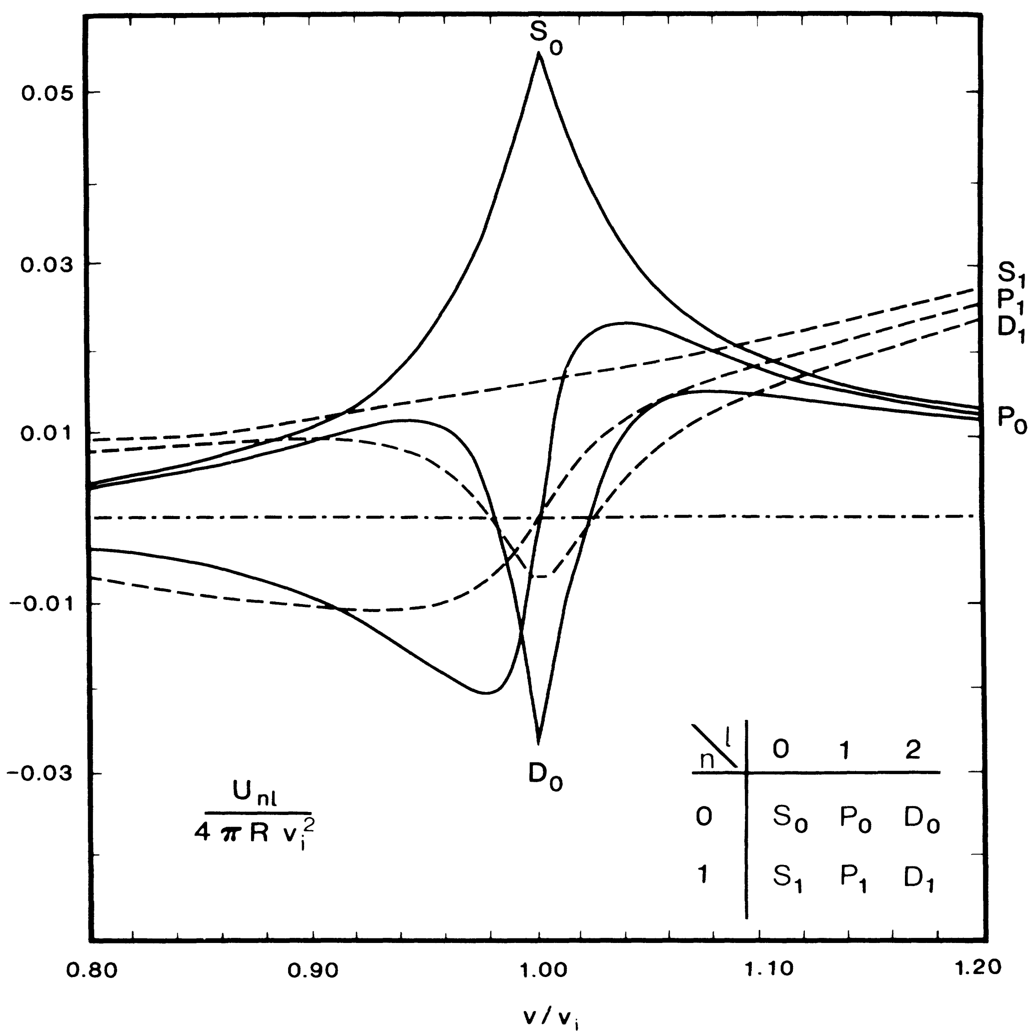

FIG. 3. Six expansion terms U_{nl} of Eq. (8) to which experimental yield spectra are fitted. These terms are exhibited here after division by $4\pi R v_i^2$ [see Eq. (A1) for definition of $L_n=U_{nl}/4\pi R v_i^2$ where $L_n=S_n$, P_n, and D_n for $l=0$, 1, and 2] so that L_n are functions of a single scaling variable $x=v/v_i$ for given acceptance angles θ_1 and θ_2 of the spectrometer. L_1 functions were multiplied by a factor of 10 for better display.

the angular acceptance of the spectrometer. For a specified spectrometer, they depend on the scaled variable $x \equiv v/v_i$ only. The cusplike behavior of S_n and D_n terms and the asymmetric character of P_n terms are well known.[13–15] Universal scaling of these terms, with respect to a single variable, emerges as a result of this work. It is evident from Fig. 3 that the $n=1$ terms are typically *one* order of magnitude smaller than the $n=0$ functions. To ascertain the importance of all terms, we have fitted experimental cusps using Eq. (8) as well as five- and even four-term expansions. Using the R^2 correlation coefficient,[19] we have established that six-term fits were indeed very good; for all spectra $0.9980 < R^2 < 0.9998$.

With five-term fits obtained by elimination of one term in Eq. (8), the deletion of U_{01} (i.e., P_0) or U_{02} (i.e., D_0) led to the worst results for H^+ and He^{2+} spectra; the elimination of P_0 was the most disastrous. As seen in Fig. 3, this was the major asymmetric term in Eq. (8), while D_0 was the main term to be influential in the wings of the cusps. Thus cusps for fully stripped projectiles *are* asymmetric. On the other hand, for the He^+ cusp the deletion of P_0 was not critical since ELC dominated this cusp and ELC spectra were apparently symmetric. This also has been noted by Gulyás *et al.* in Fig. 2 of Ref. 15. In fact, the most symmetric terms (S_0 and D_0) became the most important contributors to the cusp for the singly ionized helium. For all projectiles and target combinations, S_1 and D_1 were of least importance to the quality of the fit. A five-term fit produced by the elimination of either of these terms is essentially no different from the Eq. (8) expansion. This could be anticipated because the S_1 and D_1—originating from the $1/v_i$ terms of Eq. (5) as opposed to the $1/v'$ terms that generate the cusp peak—affected primarily the cusp wings. Gulyás *et al.*[15] simply omit the D_1 in their fit of He^{2+}-induced cusps and observe that the S_1 reflects the stability of the beam parameters rather than the true background for an ETC process. Out of the $n=1$ terms, the P_1 term has the greatest utility; especially when a fine reproduction of the cusp asymmetry is desired. Its interpretation should nevertheless be treated with caution; being important only in the wings, the P_1 term might arise because of the distortion of ETC cusps by direct ionization.[16] Inaccuracies in the subtraction of the nontarget electron yield, which are the greatest in the wing region, could also falsify the true meaning of the fitted P_1 term.

General conclusions drawn from a single-term elimination hold when four-term expansions are considered. The deletion of pairs that contain P_0 or D_0 from Eq. (8) gave significantly worse fits for fully stripped projectiles; eliminated pairs with S_0 or D_0 resulted in worse fits to He^+ cusps. On the other hand, the four-term expansions without either S_1 or D_1 were no different from the six-term fit; they were statistically identical at least on a 90% confidence level. Out of the $n=1$ terms, P_1 is the most significant because it can account in the greatest measure for asymmetries in ETC cross sections. Generally the elimination of the pairs that contained neither S_1 nor D_1 resulted in fits which could be equated with the six-term fit only at a low, 30% level of confidence.

IV. DECONVOLUTED ETC CROSS SECTIONS

We have fitted all six spectra using Eq. (8) and obtained a table of B_{nl} coefficients for these data. We present them in Table I after normalization to the coefficient B_{00} of the leading term so that their relative importance in a given spectrum can be easily recognized. We did not know the normalization of the provided yields and hence we could not extract the singly differential cross sections at the cusp peak, in terms of B_{00} as it was elegantly done at Århus University (Refs. 16 and 20). Table I exhibits, nevertheless, systematics in the relative contributions of the terms into which $d^2\sigma/dv\,d\theta$ will be expanded in Eq. (9). B_{10} and B_{12} show the largest variations from spectrum to spectrum, which supports the conclusion drawn in Sec. III that the U_{10} (i.e., S_1) and U_{12} (i.e., D_1) terms are of least significance to the quality of fit. The most asymmetric term out of the $n=1$ terms, U_{11} (i.e., P_1), has B_{11} of about order of magnitude smaller for He^+ generated spectra than for cusps induced by fully stripped ions. The importance of the asymmetric term B_{01} for fully stripped projectiles and the decisive emergence of most symmetric term B_{00} in the He^+ spectra confirm again that the asymmetry character of cusp is a good signature of the ECC mechanism while its symmetry signals a strong ELC contribution. With the exception of B_{11} for the $He^{2+} \rightarrow CH_4$ spectrum,[21] in all fits B_{01}, B_{11} and B_{02} are negative which means that for fitting purposes, in effect, the P terms are inverted and a rather deep negative dip which D_0 exhibits contributes positively to a cusp peak in the expansion of Eq. (8).

The values of the fitted B_{nl} coefficients are in general agreement with the fits performed by other[13–16]; in particular, they are consistent with the compiled B_{01} values in Ref. 16. For B_{01}, from fits to the spectra of fully stripped projectiles on CH_4 and C_3H_6, we obtain about -0.6 and -0.5. This is good agreement with other experiments for various projectiles[14,16] when scaled to our proton data, but falls somewhat below the -0.3 value that is characteristic of B_{01} coefficients found in Refs. 14–16 after their scaling to our He^{2+} results. Our $B_{01} = -0.3$ for $H^+ \rightarrow C_7H_{16}$ appears to be inconsistent with -0.6 to which all data, including ours for small hydrocarbons, appear to converge. It is known that wakes lead to a positive B_{01} in ETC from solid targets;[22] perhaps a lesser asymmetry in the largest molecular target is a signal of the wake developed in C_7H_{16}. ECC calculations for B_{01} differ so as to bracket it with too large a margin for a definitive distinction among experimental values of B_{01}. For 0.6-MeV/u H^+,He^{2+}, theoretical predictions of this asymmetry parameter range from as large as $-20/3v_i$ (i.e., -1.4 at $v_i = 4.9$),[23] through about -0.6 as calculated by Jakubassa-Amundsen (and shown in Fig. 3 of Knudsen *et al.* in Ref. 16), to as small as -0.25 (see Macek *et al.* in Ref. 8 and more recent Refs. 24 and 25). For He^+ spectra, dominated by the ELC process, we obtain $B_{01} = -0.29$ and -0.25 in CH_4 and C_7H_{16}, respectively. ELC theories[9] are more uniform than the ECC theories[8,23–25] in the predictions of B_{01}: They calculate that this anisotropy parameter in the

TABLE I. The fitted coefficients B_{nl} of Eq. (8) normalized to B_{00} which corresponds to the S_0 term, the leading term in the expansion of the cusp peak around $v'=0$. The product of B_{nl} and $(v'/v_i)^n\ P_l(\cos\theta')/v'$ gives the terms of expansion for ETC cross section [see Eq. (5) after this cross section is normalized so that its leading term equals $1/v'$].

Projectile → Molecule	B_{00}	B_{01}	B_{02}	B_{10}	B_{11}	B_{12}
$H^+ \rightarrow CH_4$	1	−0.559	−0.0842	3.528	−2.119	0.203
$H^+ \rightarrow C_3H_6$	1	−0.516	−0.0931	−1.239	−1.063	0.717
$H^+ \rightarrow C_7H_{16}$	1	−0.282	−0.1048	6.232	−5.522	1.321
$He^{2+} \rightarrow CH_4$	1	−0.575	−0.0540	−6.572	0.401	1.410
$He^{2+} \rightarrow C_7H_{16}$	1	−0.426	−0.0894	−0.216	−1.970	1.440
$He^+ \rightarrow CH_4$	1	−0.294	−0.0552	0.510	−0.455	0.575
$He^+ \rightarrow C_7H_{16}$	1	−0.245	−0.0390	−2.795	−0.266	0.187
Terms of ETC cross section [see Eq. (9)] $d^2\sigma/dv\,d\theta$	$:1/v'$	$\cos\theta'/v'$	$(3\cos^2\theta'-1)/2v'$	$1/v_i$	$\cos\theta'/v_i$	$(3\cos^2\theta'-1)/2v_i$
Terms of ETC yields [see Eq. (8)] $\frac{U_{nl}}{4\pi R v_i^2}$	$:S_0$	P_0	D_0	S_1	P_1	D_1

ELC from a 0.6-MeV/u He^+ is only very slightly negative (in a rather narrow range of $-0.1 \le B_{01} \le 0.0$). Experiments of Ref. 15 confirm these predictions in $He^+ \rightarrow He$ spectra. Our B_{01} indicates somewhat larger anisotropy, perhaps because a relatively greater fraction of ECC electrons contributes to the ETC cusps that originate from the bombardment of hydrocarbons by He^+.

Using B_{nl} of Table I we can reconstruct $d^2\sigma/dv\,d\theta$ for any v and θ, modulus a constant normalization factor, as

$$d^2\sigma/dv\,d\theta=[B_{00}+B_{01}\cos\theta'+B_{02}P_2(\cos\theta')]/v' + [B_{10}+B_{11}\cos\theta'+B_{12}P_2(\cos\theta')]/v_i\ . \quad (9)$$

This is the cross section that would be measured in the laboratory frame if no errors were to be introduced through the detection process. It should be interpreted as a generic form for any ETC doubly differential cross section, although in its original formulation [see Eq. (8) of Garibotti and Miraglia[23]] Eq. (9) was devised specifically for ECC. A multiplication of this cross section by $(v'/v)^2$ transforms it to $(d^2\sigma/dv\,d\theta)_{\rm proj}$, its value in the projectile frame. A further division by v' results in $(d^2\sigma/dE\,d\theta)_{\rm proj}=\{B_{00}+B_{01}\cos\theta' + B_{02}P_2(\cos\theta') + v'[B_{10}+B_{11}\cos\theta' + B_{12}P_2(\cos\theta')]/v_i\}/v^2$. A subsequent integration over all angles gives[26] $(d\sigma/dE)_{\rm proj} =2\pi B_{00}/E$ at $E'=0$ (Refs. 16 and 20). It is obvious[27] that for an extension of the energy spectrum of ETC cross sections beyond the tip of the cusp, i.e., to the electron energies $E'>0$ with respect to the projectile, the expansion in Eq. (5) *has* to include terms with $n>0$. In fact, the limitation to $n=1$ terms made in the existing expansions[13–16] might be too restrictive so that a reliable extraction of $d\sigma/dE$ outside the cusp neighborhood is precluded. Yet, as recalled by Burgdörfer,[24] all $n>0$ terms lead to conceptual difficulties in a meaningful comparison between experiment and theory.

Whether a singly or double differential cross section, it is its deconvoluted form that ought to be compared with theoretical predictions for ETC processes, rather than the observed yield which is distorted by finite resolution of the electron spectrometer. We will look at two aspects that characterize ETC processes and ultimately determine the shape of $d^2\sigma/dv\,d\theta$ as a function of the electron speed at selected θ angles. The shape of the ETC cross section can be delineated in terms of (i) the asymmetry or lack thereof for this cusplike cross section, (ii) the full width at half maximum (FWHM) normalized to v at the cusp maximum, i.e., $(\Delta v/v)_{\rm FWHM}$. Ideally, both these aspects should be experimentally studied as functions of the average acceptance angle θ_0 and ion velocity v_i. All spectra at our disposal were produced at the same θ_0 and v_i and thus we cannot make any statements on the dependence of asymmetry or of width on these variables. Nevertheless, the extracted cross section of Eq. (9) can be investigated as a function of the ejected electron speed v and scattering angle θ. We therefore, after a quantitative discussion of the observed asymmetry in the provided spectra, will examine ETC electrons before their velocity distribution is altered upon the entrance into electron spectrometers from spatially extended interaction regions.

As a measure of asymmetry we define A, a ratio of counts on the low-velocity side of the peak maximum to the number of counts on its high-velocity side. Counts collected in the peak channel are halved and as such added to all counts in the channels below and above the peak channel. For the provided spectra,[18] the empirical values of A were 2.0 for fully stripped projectiles and 1.1 for the singly ionized helium ions. The skewness systematics mentioned in the Introduction are very well manifested by these data: Bare projectiles result in distinctly asymmetric peaks, while He^+ ions yield nearly symmetric cross sections around $v'=0$. These characteristics are consistent with the notion that ELC processes, which on theoretical grounds give rise to symmetric or nearly symmetric cross sections, dominate over the ECC mechanism when the bombarding projectile comes with an electron. Conclusions drawn in this paragraph on the basis of experiment apply similarly to our fitted cusps of Eq. (8) since these fits faithfully reproduce the data. The fitted cusps, however, offer a distinct advantage in the definition of the asymmetry factor. One can determine A more adequately through numerical integration of the fitted cusps below and above $v/v_i=1$: An ambiguous assignment of the peak channel counts to the left and right sides of the peak does not have to be made. We have calculated A for all spectra as the ratio of fitted cusps integrated over the 0.9–1.0 and 1.0–1.1 ranges of v/v_i; the 0.1 interval in v/v_i on both sides of the fitted peaks corresponds to the range of channels over which the analyzed cusps were measured. There was no systematic dependence of A on the target composition and this asymmetry factor did depend on the nature of the projectile. The upper band in Fig. 4 covers all A's for fully stripped projectiles which produced cusps with the significant asymmetry. The lower band brackets the asymmetry factor in He^+ generated cusps where the ELC masks the asymmetry that are so indicative of ECC processes. Such a correlation of the skewness with the charge state of the projectile has been observed and explained before.[6–11]

We can now obtain a deeper and more revealing understanding of the asymmetry by stripping the observed cusps of the instrumental distortion introduced by the electron spectrometer and finite extension of the ETC interaction region. Equation (9) allows us to investigate the asymmetry of $d^2\sigma/dv\,d\theta$ as a function of θ. Figure 4 reveals that for typical spectra in which θ is at most a few degrees, the asymmetry originates at the angles that are small relative to θ_0. The only exception was the skewness of $d^2\sigma/dv\,d\theta$ extracted from the $He^{2+}\rightarrow CH_4$ spectrum; its A hovered around a factor of 3 for all angles θ. We attribute this anomaly to errors in the provided spectrum;[21] the A of $He^{2+}\rightarrow CH_4$ deconvoluted is not shown in Fig. 4. An analysis of the asymmetry systematics in the extracted $d^2\sigma/dv\,d\theta$ for all other provided spectra, illustrated in Fig. 4, suggests that is more symmetric ELC cusps the asymmetry dependence on θ is less pronounced. This behavior of ETC cross sections as a function of the scattering angle θ has not been mentioned in studies of experimental cusps. It escaped previous notice because the observed cusps are composites of the $d^2\sigma/dv\,d\theta$ cross section convoluted with an instrumental tranmission that filters through the most forward-ejected electrons. The skewness of calculated ETC cross sections remains a useful quantity in the taxonomy of experimental cusp spectra because spectrometers do not critically affect the most forward-scattered electrons that shape observed cusps. Nevertheless, an intercomparison of the skewness in ETC spectra—taken for the same collision systems but with different detection systems—requires *a priori* extraction of the ETC cross sections from such data.

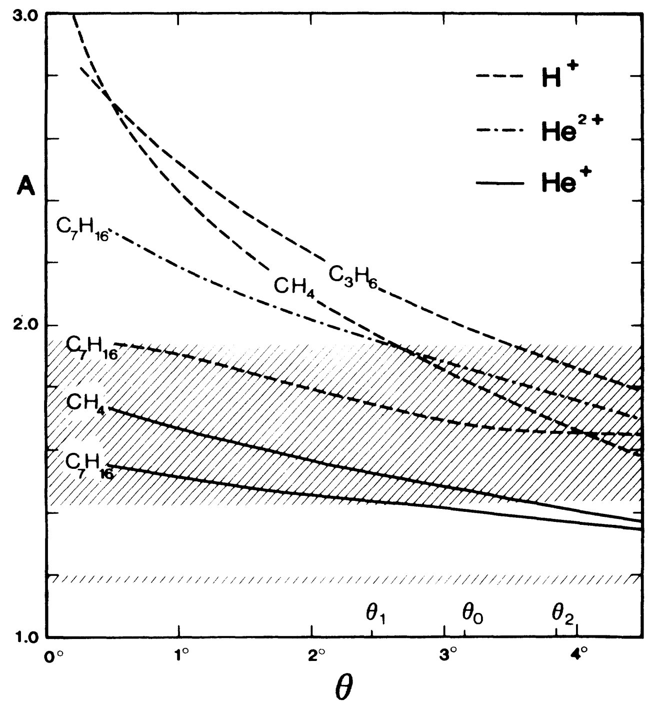

FIG. 4. Asymmetry factor A defined in the text as a ratio of the low-velocity to the high-velocity side of deconvoluted cusps vs the scattering angle θ. The shaded bands bracket A values for fully stripped (upper band) and hydrogenic projectiles (lower band) are based on the fitted cusps to the observed spectra; these A's represent the asymmetry of ETC cusps prior to their deconvolution and as such are θ independent. The deconvoluted cross sections $d^2\sigma/dv\,d\theta$ of Eq. (9) show that the asymmetry originates at small scattering angles. The dashed curves for fully stripped ions demonstrate that this behavior is particularly symptomatic of ECC mechanism as contrasted with the solid curves for He^+ which—as a hydrogenic projectile—predominantly contributes to ETC through ELC processes that are more symmetric.

The deconvoluted cusp, free of the instrumental bias, gives also a more probing understanding of the relative width behavior in electron cusps. Prior to the deconvolution, the cusps—based on an analysis of observed count versus channel distributions—had $(\Delta v/v)_{FWHM}$ which ranged from 0.058 to 0.064. A more adequate analysis based on the fitted spectra gives $(\Delta v/v)_{FWHM}$ in the 0.056 to 0.082 range (see the shaded band in Fig. 5). The relative widths did not exhibit systematic dependence nor significant difference among the various projectile-target combinations. Their values gravitated around $2R=0.06$, i.e., the instrumental full width at half maximum of the spectrometer's $V(v)$. Conventional studies involve $(\Delta v/v)_{FWHM}$ as a function of θ_0, and center around the prediction by Dettmann[17] that

$(\Delta v/v)_{\mathrm{FWHM}} = 1.5\theta_0$. For our spectra (with $\theta_0 = 0.0545$ rad), Dettmann's formula gives $(\Delta v/v)_{\mathrm{FWHM}} = 0.082$, which is in agreement with the $(\Delta v/v)_{\mathrm{FWHM}}$ that we have obtained from the fitted spectra. However, the validity of making direct and absolute comparisons between experimental widths and theoretical predictions might be questioned. Such comparisons are always problematical when the relative cusp widths $(\Delta v/v)_{\mathrm{FWHM}}$ are not much less than $2R$;[28] for spectra analyzed in this work, the relative width is comparable to $2R$. The $R = 0.03$ resolution could impose stringent limits as to how wide the observed peaks are. Such an instrumental resolution eliminates the ETC electrons of relatively large velocity spread; production of these electrons could be critically dependent on the mechanism of the electron transfer to the projectile's continuum.

Thus it is instructive to look in Fig. 5 at $(\Delta v/v)_{\mathrm{FWHM}}$

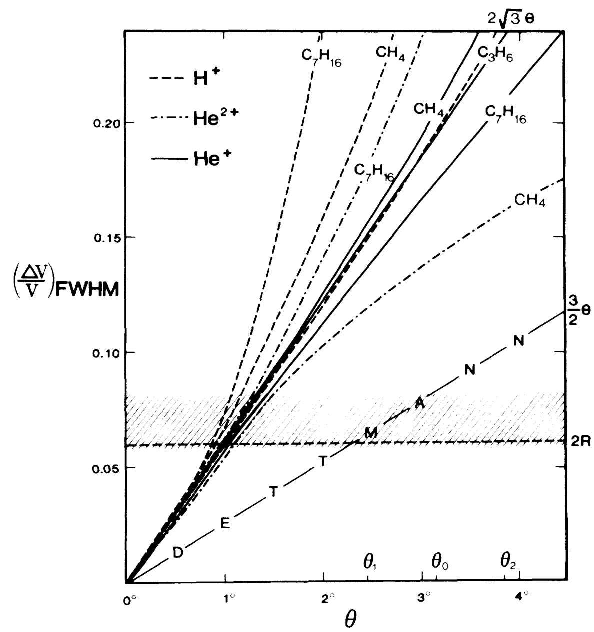

FIG. 5. Velocity full width at half maximum, Δv_{FWHM}, relative to the velocity at the peak maximum vs the scattering angle θ. Spectra for all projectile-target combinations have $(\Delta v/v)_{\mathrm{FWHM}}$ within a relatively narrow range of values (shown by the shaded band) because of the common and critical imprint of the spectrometer whose $2R$ resolution was 0.06. These relative widths are in basic agreement with Dettmann's prediction of Ref. 17, in which θ is set at the conventional acceptance angle θ_0 (3.12° for the experimental arrangement of Ref. 18) and only B_{00}/v' is assumed to calculate the width of experimental cusps. The widths of deconvoluted cusps, the dashed curves for fully stripped projectiles and solid curves for singly ionized helium, indeed converge in the small-angle approximation to the line marked $2\sqrt{3}\theta$, which is the calculated $(\Delta v/v)_{\mathrm{FWHM}}$ for a $1/v'$ cross section. At angle larger than 1°, the width of the deconvoluted cross sections vs θ diverges from this line. This split could be indicative of the difference between ECC and ELC cross sections, the width difference that is masked in experimental cusps by the relatively narrow velocity resolution of the spectrometer.

in $d^2\sigma/dv\,d\theta$ of Eq. (9) plotted versus θ. We could fit the relative widths of all deconvoluted spectra to $(\Delta v/v)_{\mathrm{FWHM}} = (3.3\pm0.2)\theta$ for $\theta < 0.0175$ rad $= 1°$. For $\theta > 1°$, $(\Delta v/v)_{\mathrm{FWHM}}$ versus θ diverges from a straight-line dependence to different degrees for different projectile-target combinations (see Fig. 5). In the small-angle limit, all ETC cross sections converge to B_{00}/v', which is the leading term of the expansion in Eq. (9). The relative full-width at half-maximum for this term is $2\sqrt{3}\tan\theta$. For angles less than a few degrees (this means for all θ in Fig. 5), this formula is very well approximated by the straight line marked $2\sqrt{3}\theta$. In fact, Dettmann's $1.5\theta_0$ obtains only in this linear approximation to $(\Delta v/v)_{\mathrm{FWHM}}$ for the convoluted cusp. The relative widths of our deconvoluted spectra indeed converge to the $2\sqrt{3}\theta$ line for $\theta < 1°$. At larger angles, the terms *other* than B_{00}/v' begin to influence the width $(\Delta v/v)_{\mathrm{FWHM}}$. Neglecting the $He^{2+} \rightarrow CH_4$ curve since it was based on inaccurate spectrum,[21] it appears that ECC cross sections due to fully stripped projectiles (dashed curves in Fig. 5) are characterized at larger angles by somewhat wider width than the width of the leading term. By contrast, the width of the ELC cross sections ($He^{+} \rightarrow CH_4$, C_7H_{16} solid curves in Fig. 5) rises less steeply with the increasing θ. Such a statement is more speculative, however, since residual ECC contributions could hinder this trend. Note that the leading term of Eq. (9), to which all extracted cross sections converge in the limit of the small acceptance angle, generates a cusp whose width is predicted by Dettmann's theory.[17] If the velocity resolution of the electron spectrometer were significantly wider than $(\Delta v/v)_{\mathrm{HWHM}} = R = 0.03$ for the presently analyzed data, the observed cusp width could result in a substantial disagreement with the Dettmann's prediction and the width of this cusp would be more sensitive to the nature of the projectile-target system. The narrow transmission window in speed allows preferentially for small ($\theta < 1°$) angle contributions to the cusp; since the leading term becomes increasingly important as $\theta \rightarrow 0$, all observed spectra are in essence dominated by this term, i.e., they exhibit similar widths (as covered by the shaded band of Fig. 5). Hence—irrespectively of ETC mechanisms and contrary to the very recent claim[29]—$1.5\theta_0$ agrees excellently with $(\Delta v/v)_{\mathrm{FWHM}}$ of *convoluted* cusps.

V. CONCLUSIONS

We have fitted the provided cusp spectra with a six-term expansion into characteristic functions, which were derived analytically after the introduction of analytical approximations for the transmission function in the detection of ETC electrons. Criteria for goodness of fit were established using the R^2 method of statistical analysis. A discussion of optimal expansions for the fitting of experimental yields was made. The significance of various terms in such expansions was determined.

The fitting coefficients from a linear least-squares program[12] allowed for reconstruction of the deconvoluted ETC spectrum, $d^2\sigma/dv\,d\theta$, as a generic ETC cross section which—being free of instrumental distortions—could be compared directly with theoretical predictions for ECC and ELC processes. Extracted ETC cross sections gave a better understanding of the origin of cusp asymmetry in these processes. We discovered that contributions to asymmetry come at small angles ($\theta < \theta_0$). Deconvoluted ETC spectra gave also a better understanding of widths in the observed cusps. We have found that the experimental velocity transmission window affects the data by filtering through highly forward scattered electrons and thus resulting in the cusps of appreciably narrower widths than expected from $d^2\sigma/dv\,d\theta$. Widths of ETC cross sections are truncated by the spectrometer so as to obscure the difference between ECC and ELC cross sections.

A comment on the existence of wakes in molecules can be made in view of our findings. We note that the deconvoluted spectra had widths which were proportional to θ, at least in small-angle approximation. In fact, the widths converge to zero when $\theta \rightarrow 0°$. This could prevent speculation[3] on the possible wake-state origin of the ETC electrons from molecular targets since the wake theory predicts[30] that the width should be θ independent. It has been recently discovered by Elston *et al.*[31] that wakes are signified by the presence of high-l contributors in Eq. (5). By limiting our analysis to $l \leq 2$, we might have forcefully mislabeled high-multipole contributions of wakes. If wakes were to arise, the D terms would be most sensitive to their existence in such a restrictive analysis. Except for the He^+ spectra, in which ELC overshadows possible evidence for wakes, Table I indeed displays the enhancement of the B_{n2} terms when larger molecules are analyzed. As we have mentioned in a discussion of B_{01}, the formation of wakes in C_6H_{17} might explain $B_{01} = -0.3$ as contrasted with -0.6 in CH_4. These results support an affirmative answer to the question posed in Refs. 2 and 3 on the wake formation in large hydrocarbon molecules.

A comparison of the findings about characteristics of $d^2\sigma/dvd\theta$, that were inferred here from deconvoluted cusp spectra, with the direct measurements of the doubly differential ETC cross section—which become available in a new generation of experiments that map experimental contours of $d^2\sigma/dv\,d\theta$ in the v-θ plane[31]—would be of interest. We hope that our results, codified in an expansion series with identification of critical and characteristic terms, will serve as a stimulus for further theoretical investigation into the shape and origins of the ETC cusp. It is our expectation that further systematic measurements of the cusp shape (especially as a function of the collection angle) and their analysis with analytical formulas that account for a variety of possible instrumental resolutions, will provide more insight into the nature of the ETC cusp asymmetry and its width. Known difficulties in making a comparison between convoluted data taken at different laboratories have been reiterated recently by Man *et al.*[32] Deconvoluted cross sections are needed. Experiments for identical collisions, performed with spectrometers of different resolution, can be compared as equivalent once the observed yields are stripped of the distortions caused by the detection process. Theoretical predictions—for example, from ETC viewed as an electron transfer to high Rydberg states extrapolated into the continuum[33]—could be compared directly with the deconvoluted cross section. The unfolded data may be tested against doubly differential measurements and theories for ETC cross sections; mechanisms for the electron transfer to the projectile's continuum should hence be better understood.

We plan to extend the utility of the Meckbach *et al.* deconvolution procedure[13] by supplementing the derived analytical functions U_{nl} ($n=0,1$, $l=0,1,2$) with U_{nl} for larger n and l. The $n>1$ functions are desired to extract ETC cross sections beyond their cusp peak value, while the $l>2$ functions should be pivotal for a firm conformation of the existence of wakes in large-size molecules and for a systematic investigation of the multipole wake content in solid targets.

This paper is based on thesis presented by Y. C. Yu in partial fulfillment of the requirements for the degree of Master of Science in Physics at East Carolina University.

APPENDIX: ANALYTICAL FUNCTIONS, $U_{nl} = 4\pi R v_i^2 L_n$, FOR FITS TO ETC SPECTRA

With $\Theta(\theta)$ of Eq. (4), U_{nl} of Eq. (7) can be written as $U_{nl} = 4\pi R v_i^2 L_n$ in terms of

$$L_n \equiv L_n^0(1;x) - L_n^0(\mu_1;x) + \sum_{j=0}^{2} a_j [L_n^j(\mu_1;x) - L_n^j(\mu_2;x)] \,, \tag{A1}$$

where L_n, with v' and θ' defined below Eq. (5), are the integrals

$$L_n^j(\mu;x) = x^3 \int (v'/v_i)^{n-1} (\cos\theta)^j P_l(\cos\theta')\, d(\cos\theta) \tag{A2}$$

with $L=S$, P and D for $l=0,1,2$. The $L_n(\mu;x)$ are functions of $\mu \equiv \cos\theta$ and $x = v/v_i$. The integrals of Eq. (A2) were calculated analytically in Appendixes B and C of Ref. 12. We show L_n of Eq. (A1) in Fig. 3 and reproduce them in this appendix without the derivation which was presented in Ref. 12. Below we list the formulas for $L_n^j(\mu;x)$ in terms of $y \equiv (1+x^2-2\mu x)^{1/2}$ so that these formulas can be displayed compactly; at $x=\mu$ the ETC cross section of Eq. (5) exhibits peaking behavior. The formulas for six L_n^j's with $n=0,1$ and $L=S$, P, and D are grouped in the following according to the j superscript. Note that only the $j=0$ integrals would be needed if the angular acceptance function Θ were to be approximated by the step function.

$j=0$ integrals

The $j=0$ integrals include the following:

$$S_0^0 = -x^2 y \,,$$

$$P_0^0 = -x^2[x\mu - (1-x^2)\ln y]/2 \,,$$

$$D_0^0 = -x^2[y^3 + 2(1-3x^2)y - 3(1-x^2)^2/y]/8 \,,$$

$$S_1^0 = x^3\mu \,,$$

$$P_1^0 = x^2[y^3/3 + (1-x^2)y]/2 \,,$$

$$D_1^0 = -x^2[3y^4 - 8(1-3x^2)x\mu + 12(1-x^2)^2 \ln y]/32 \,.$$

$j=1$ integrals

The $j=1$ integrals include the following:

$$S_0^1=-x(1+x\mu+x^2)y/3\ ,$$

$$P_0^1=-x\{x^2\mu^2-(1-x^2)[x\mu+(1+x^2)\ln y]\}/4\ ,$$

$$D_0^1=-x[3(1+3x\mu+x^2)y^3+10(1+x\mu+x^2)(1-3x^2)y-45(1-x\mu+x^2)(1-x^2)^2/y]/120\ ,$$

$$S_1^1=x^3\mu^2/2\ ,$$

$$P_1^1=x[(1+3x\mu+x^2)y^3+5(1-x^2)(1+x\mu+x^2)y]/30\ ,$$

$$D_1^1=x\{y^6-1.5(1+x^2)y^4+4(1-3x^2)x^2\mu^2-6(1-x^2)^2[x\mu+(1+x^2)\ln y]\}/32\ .$$

$j=2$ integrals

The $j=2$ integrals include the following:

$$S_0^2=-[3x^2\mu^2+2x\mu(1+x^2)+2(1+x^2)^2]y/15\ ,$$

$$P_0^2=-x^3\mu^3/6-(1-x^2)[(1+x^2)y^2-y^4/4-(1+x^2)^2\ln y]/8\ ,$$

$$D_0^2=-\{3[15x^2\mu^2+6(1+x^2)x\mu+2(1+x^2)]y^3+14[3x^2\mu^2+2(1+x^2)x\mu+2(1+x^2)^2](1-3x^2)y-105[0.75(1+x^2)^2+1.5(1+x^2)y^2-0.25y](1-x^2)^2/y\}/840\ ,$$

$$S_1^2=x^3\mu^3/3\ ,$$

$$P_1^2=-[15x^2\mu^2+6(1+x^2)x\mu+2(1+x^2)^2]y^3/210+(1-x^2)[3x^2\mu^2+2x\mu(1+x^2)+2(1+x^2)^2]y/30\ ,$$

$$D_1^2=-\{1.5y^8-4(1+x^2)y^6+3(1+x^2)^2y^4-32(1-3x^2)x^3\mu^3/3+3(1-x^2)^2\times[y^4-4(1+x^2)y^2+4(1+x^2)^2\ln y]\}/128\ .$$

---

* Present address: Department of Physics, North Texas State University, Denton, Texas 76203.

[1] A. Gladieux and A. Chateau-Thierry, Phys. Rev. Lett. **47**, 786 (1981).
[2] G. Bissinger, J. Gaiser, J. M. Joyce, G. Lapicki, and M. Numan, Bull. Am. Phys. Soc. **29**, 814 (1984).
[3] G. Bissinger, J. Gaiser, J. M. Joyce and M. Numan, Phys. Rev. Lett. **55**, 197 (1985).
[4] M. E. Rudd, C. A. Sauter, and C. L. Bailey, Phys. Rev. **151**, 20 (1966); **151**, 28 (1966); G. B. Crooks and M. E. Rudd, Phys. Rev. Lett. **25**, 1599 (1970); K. G. Harrison and M. Lucas, Phys. Lett. A **33**, 142 (1970); J. Macek, Phys. Rev. A **1**, 235 (1970).
[5] W. Meckbach and R. A. Baragiola, in *Inelastic Ion-Surface Collisions,* edited by N. M. Tolk, J. C. Tully, W. Heiland, and C. W. White (Academic, New York, 1977), p. 283; I. A. Sellin, J. Phys. (Paris) **40**, C1 (1979); C. R. Vane, IEEE Trans. Nucl. Sci. **26**, 1078 (1979); M. W. Lucas, in *Proceedings of the Workshop on Physics with Fast Molecular-Ion Beams,* edited by D. S. Gemmell, Argonne, 1979 [Argonne National Laboratory Report No. ANL/PHY-79-3, 1979, p. 291]; V. H. Ponce and W. Meckbach, Comments At. Mol. Phys. **10**, 231 (1981); M. Breining, S. B. Elston, S. Huldt, L. Liljeby, C. R. Vane, S. D. Berry, G. A. Glass, M. Schauer, I. A. Sellin, G. D. Alton, S. Datz, S. Overbury, R. Laubert, and M. Suter, Phys. Rev. A **25**, 3015 (1982); I. A. Sellin, in *Proceedings of the Twelfth International Conference on the Physics of Atomic and Electron Collisions, Gatlinburg, 1981,* edited by S. Datz (North-Holland, Amsterdam, 1982), p. 195; *Forward Electron Ejection in Ion Collisions,* Vol. 213 of *Lecture Notes in Physics,* edited by K. O. Groenveld, W. Meckbach, and I. A. Sellin (Springer, Berlin, 1984); K. O. Groenveld, W. Meckbach, I. A. Sellin, and J. Burgdörfer, Comments At. Mol. Phys. **14**, 187 (1984).
[6] C. R. Vane, I. A. Sellin, M. Suter, G. D. Alton, S. B. Elston, P. M. Griffin, and R. S. Thoe, Phys. Rev. Lett. **40**, 1020 (1978).
[7] M. Rødbro and F. D. Andersen, J. Phys. B **12**, 2883 (1979).
[8] R. Shakeshaft and L. Spruch, Phys. Rev. Lett. **41**, 1037 (1978); J. Macek, J. E. Potter, M. M. Duncan, M. G. Menendez M. W. Lucas, and W. Steckelmacher, *ibid.* **46**, 1571 (1981); D. H. Jakubassa-Amundsen, J. Phys. B **16**, 1767 (1983).
[9] J. S. Briggs and F. Drepper, J. Phys. B **11**, 4033 (1978); J. S. Briggs and M. H. Day, *ibid.* **13**, 4797 (1980); M. H. Day, *ibid.*, **14**, 231 (1981); J. Burgdörfer, J. Phys. B **19**, 417 (1986).
[10] M. Breinig, M. M. Schauer, I. A. Sellin, S. B. Elston, C. R. Vane, R. S. Thoe, and H. Suter, J. Phys. B **14**, 1291 (1981).
[11] M. G. Menendez, M. M. Duncan, F. L. Eisele, and B. R. Junker, Phys. Rev. A **15**, 80 (1977); R. W. Cranage, W. Steckelmacher, and M. W. Lucas, Nucl. Instrum. Methods **194**, 419 (1982); K. F. Man, W. Steckelmacher, and M. W. Lucas, J. Phys. B **19**, 401 (1986).
[12] Y. C. Yu, Master of Science thesis, East Carolina University, 1986 (unpublished).
[13] W. Meckbach, I. B. Nemirovsky, and C. R. Garibotti, Phys. Rev. A **24**, 1793 (1981).
[14] S. D. Berry, G. A. Glass, I. A. Sellin, K. O. Groenveld, D. Hofmann, L. H. Andersen, M. Breing, S. B. Elston, P. Engar, M. M. Schauer, N. Stolterfoht, H. Schmidt-Böcking, G. Nolte, and G. Schweitz, Phys. Rev. A **31**, 1392 (1985).
[15] A. Köver, G. Szabó, D. Berényi, L. Gulyás, I. Cserny, K. O. Groenveld, D. Hofmann, P. Koschar, and M. Burkhard, J. Phys. B **19**, 1187 (1986); L. Gulyás, G. Szabó, D. Berényi, A. Köver, K. O. Groenveld, D. Hofmann, and M. Burkhard,

Phys. Rev. A **34**, 2751 (1986).

[16]L. H. Andersen, K. E. Jensen, and H. Knudsen, J. Phys. B **19**, L161 (1986); H. Knudsen, L. H. Andersen, and K. E. Jensen, *ibid.*, **19**, 3341 (1986).

[17]K. Dettmann, Proceedings of the Conference on Interactions of Energetic Charged Particles in Solids, Istanbul, 1972 [Brookhaven National Laboratory Report No. BNL 50336 (1972)] (unpublished); K. Dettmann, K. G. Harrison, and M. W. Lucas, J. Phys. B **7**, 269 (1974).

[18]The provided electron spectra are from 1985 experiments of G. Bissinger, J. Gaiser, and J. M. Joyce on a 2-MV Tandem Van de Graaff Accelerator at East Carolina University (unpublished).

[19]M. R. Spiegel, *Schaum's Outline Series: Theory and Problems of Statistics* (McGraw-Hill, New York, 1981).

[20]P. Dahl, J. Phys. B **18**, 1181 (1985).

[21]All provided spectra were corrected for out-of-target contributions *prior* to their deconvolution. As explained in Ref. 3—to achieve the same beam-line vacuum—target gases were bleeded into the target chamber and their measured contribution was subracted from the spectra with the gas in the target cell. This background subtraction procedure affected the $He^{2+} \rightarrow CH_4$ spectrum to the largest degree; thus we do not consider these data as a reliable input for our analysis. Note that errors due to this background subtraction are minimized when only *differences* between spectra are analyzed as it was done in Ref. 3.

[22]M. W. Lucas, W. Steckelmacher, J. Macek, and J. E. Potter, J. Phys. B **13**, 4833 (1980); S. B. Elston, I. A. Sellin, M. Breining, S. Huldt, L. Liljeby, R. S. Thoe, S. Datz, and S. Overbury, Phys. Rev. Lett. **46**, 321 (1981).

[23]C. R. Garibotti and J. E. Miraglia, J. Phys. B **14**, 863 (1981).

[24]J. Burgdörfer, Phys. Rev. A **33**, 1578 (1986).

[25]D. S. F. Crothers and J. F. McCann, J. Phys. B **20**, L19 (1987); see also p. 598 in Ref. 29.

[26]In Refs. 16 and 20 $(d^2\sigma/dEd\theta)_{\rm proj}$, rather than the cross section that is differential with respect to the velocity of the transferred electron and expressed in the laboratory frame (see Refs. 12–15), was expanded around $E'=0$. This gives a different meaning to the B_{nl} coefficients. In particular, at $E'=0$ $(d\sigma/dE)_{\rm proj}=4\pi B_0^0$ using the B_l^n coefficients. In our work, all B_{nl} have the dimension of the cross section and $(d\sigma/dE)_{\rm proj}=2\pi B_{00}/E$ is dimensionally consistent with the units of B_{nl}. The cusp height at its maximum, obtained after the angular integration, is explicitly shown to be inversely proportional to the laboratory energy of the electrons that appear at this peak.

[27]J. E. Miraglia and V. H. Ponce, J. Phys. B **13**, 1193 (1980).

[28]K. R. Chiu, W. Meckbach, G. Sanchez Scarimento, and J. W. McGowan, J. Phys. B **12**, L147 (1979).

[29]S. Y. Ovchinnikov and D. B. Khrebtukov, in *Contributed Papers of the Fifteenth International Conference on the Physics of Electronic and Atomic Collisions, Brighton, 1987,* edited by J. Geddes, H. B. Gilbody, A. E. Kingston, C. J. Latimer, and H. J. R. Walters (The Queen's University, Belfast, 1987), p. 596. Dettman's curve is drawn about 50% below the measured widths of Ref. 15. Köver *et al.* noted, however, that both ECC and ELC cusps were in perfect agreement with Dettmann's formula evaluated at 1.5° that was an effective half-angle of acceptance in their experiments.

[30]W. Brandt and R. H. Ritchie, Phys. Lett. **62A**, 374 (1977).

[31]S. B. Elston, in *Invited Papers of the Fourteenth International Conference on the Physics of Electronic and Atomic Collisions, Palo Atlo, 1985,* edited by D. C. Lorents, W. E. Meyerhof, and J. R. Peterson (North-Holland, Amsterdam, 1986), p. 331; S. D. Berry, S. B. Elston, I. A. Sellin, M. Breinig, R. de Sario, C. E. Gonzalez-Lepera, and L. Liljeby, J. Phys. B **19**, L149 (1986); S. B. Elston, Nucl. Instrum. Methods **B24/25**, 214 (1987).

[32]K. F. Man, W. Steckelmacher, and M. W. Lucas, J. Phys. B **19**, 4171 (1986).

[33]O. Schöller, J. S. Briggs, and R. M. Dreizler, J. Phys. B **19**, 2505 (1986); L. J. Dubé and A. Salin, *ibid.* **20**, L499 (1987).